this basis the first excited state would be a 2+ state, and the conversion coefficient for the gamma transition would be about 500. Other excited states similar to those of Cm^{242} would be in too low intensity for observation with the preparations now available.

We wish to acknowledge the assistance of Miss Beverly Turner and Mrs. Marjorie Simmons in counting the alpha tracks. We would like to acknowledge the use of the pile facilities and the aid of the personnel of the Atomic Energy Project, National Research Council of Canada, Chalk River, Ontario, Canada, in the irradiations of plutonium, americium, and curium. This work was performed under the auspices of the U. S. Atomic Energy Commission.

PHYSICAL REVIEW VOLUME 92, NUMBER 3 NOVEMBER 1, 1953

Slow Neutron Velocity Spectrometer Studies. V. Re, Ta, Ru, Cr, Ga

E. MELKONIAN, W. W. HAVENS, JR., AND L. J. RAINWATER
Columbia University, New York, New York

(Received July 31, 1953)

New developments in the analysis of data near resonance levels are described. These allow more accurate values of the level constants to be determined from the measured areas above transmission curves and are more general in their applications. The effect of Doppler broadening is also taken into consideration. Transmission data on Re, Ta, Ru, Cr, and Ga are presented. The thermal region of Re is well matched by the relation $\sigma=5.0+15.8E^{-\frac{1}{2}}$. Resonances are found in Re at 2.18, 4.40, 5.92, 7.18, 11.3, 13.1, 17.7, and 21.1 ev. The strong level at 2.18 ev has been studied by the technique of using two samples of different thickness, giving $\sigma_0=5700$ barns and $\Gamma=0.090$ ev. The method of curve fitting was also applied to the transmission dip of the thick sample at 2.18 ev and confirms the values of σ_0 and Γ from the area method. Curve fitting was also used on the 4.40-ev level. New data for Ta in the region above 5 ev are presented. Some transmission dips thought previously to be due to one level have now been resolved into two levels. There are levels at 6.11, 10.2, 13.7, 20.0, 24.0, 35.1, and 38.2 ev. The thermal region of Ru is well matched by the relation $\sigma=6.4+0.39E^{-\frac{1}{2}}$. Resonance levels are observed at 9.8, 15.2, 24.1, and 40.9 ev. The thermal region of Cr is well matched by the relation $\sigma=3.8+0.7E^{-\frac{1}{2}}$. A resonance level is observed at 3800 ev. The nuclear cross section of Ga is given by $\sigma=7.3+0.35E^{-\frac{1}{2}}$ below 5 ev. In addition interference effects occur in the thermal region. Levels were found at 102 ev and 310 ev, with indications of levels at higher energies.

INTRODUCTION

THE results of previous investigations using the Columbia University slow neutron velocity spectrometer have been presented in a series of earlier papers.[1–3] The present paper is the fifth of a series[2] which presents the results of survey studies of nuclear resonance levels. The improvements and re-evaluation described in the fourth paper[2] apply here. In addition, some new developments in the analysis of data near resonance levels are presented and applied to the data of this report.

Analysis of Resonance Level Parameters

Techniques for obtaining information about the parameters σ_0 and Γ of a neutron resonance from the experimental transmission curve have been described in previous reports.[1–3] It has been repeatedly pointed out that in the vicinity of a resonance, it is not usually possible to obtain the cross section σ from the experimental transmission T by using the formula $T=e^{-n\sigma}$, where n is the number of atoms per cm^2 in the sample. The authors find, however, that there seems to be a strong tendency to give direct significance to the curve of σ *vs* E obtained in this manner,[4] in spite of the warning to the contrary given in the introduction to this compilation. It should be stressed that such a curve of σ *vs* E has little meaning in the region of a resonance level unless the instrumental resolution width is small compared to the level width. In most cases the maximum σ obtained in this manner is small compared to the true σ_0 and decreases with increasing thickness of sample. In certain favorable cases, where $n\sigma_0$ is not large and the level width is not small compared to the resolution width, trial values of level parameters may be chosen and the calculated expected transmission curve (including the effect of the instrumental resolution width) compared with the experimental transmission curve. In especially suitable cases, this may be done in the final stage of the analysis.

As has been pointed out previously, the determination of the level parameters is frequently possible only by an analysis of the area, defined below, of the trans-

[1] L. J. Rainwater and W. W. Havens, Jr., Phys. Rev. **70**, 136 (1946); W. W. Havens, Jr., and L. J. Rainwater, Phys. Rev. **70**, 154 (1946).

[2] (I) Rainwater, Havens, Wu, and Dunning, Phys. Rev. **71**, 65 (1947); (II) Havens, Wu, Rainwater, and Meaker, Phys. Rev. **71**, 165 (1947); (III) Wu, Rainwater, and Havens, Phys. Rev. **71**, 174 (1947); (IV) W. W. Havens, Jr., and L. J. Rainwater, Phys. Rev. **83**, 1123 (1951).

[3] Rainwater, Havens, Dunning, and Wu, Phys. Rev. **73**, 733 (1948); Havens, Rainwater, Wu, and Dunning, Phys. Rev. **73**, 963 (1948).

[4] *Neutron Cross Sections*, Atomic Energy Commission Report AECU-2040 (U. S. Government Printing Office, Washington (1952)).

mission dip in the vicinity of the resonance. This method is particularly valuable when the resolution function is not well-known.

In using the Breit-Wigner one-level formula, we adopt the usual simplifying conditions: (1) the interference term between potential and resonance scattering is neglected, and (2) $\Gamma/E_0 \ll 1$, so that $(E_0/E)^{\frac{1}{2}} \approx 1$ over the level.

Then

$$\sigma = \sigma_{\text{const}} + \sigma_r,$$
$$\sigma_r = \sigma_0\{1+[2(E-E_0)/\Gamma]^2\}^{-1},$$
$$T = (T_{\text{const}})(T_r) = (e^{-n\sigma_{\text{const}}})(e^{-n\sigma_r}).$$

If σ_{const} is evaluated in some way,[3] the experimental transmission curve may be divided by T_{const} to give T_r (experimental). For a strong resonance and a thin sample, $T_{\text{const}} \approx 1$ and the correction may be neglected. The "areas" A_E and A_t are defined as

$$A_E = \int_{-\infty}^{\infty} (1-T_r)dE,$$

if an energy abscissa is used, and

$$A_t = \int_{-\infty}^{\infty} (1-T_r)dt,$$

if a time-of-flight abscissa is used. If $\Gamma/E_0 \ll 1$, then $A_t = A_E(t_0/2E_0)$ is a good approximation and will be used in the following analysis. Subsequent developments will be in terms of A_E since simpler expressions are obtained. However, A_t is generally measured when time-of-flight techniques are used, and the above formula must be used to obtain A_E. It should be noted that any analysis which makes use of the area above a resonance dip depends upon the fact that this area is independent of the resolution function of the measuring equipment, provided of course, that this function is reasonably well-confined.

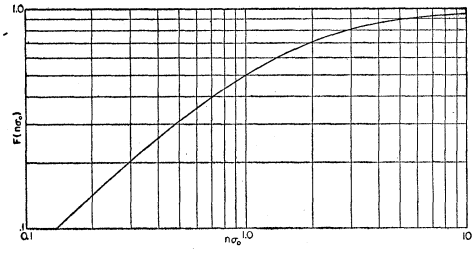

FIG. 1.

$$F(n\sigma_0) = \frac{1}{4\pi n\sigma_0}\left[\int_{-\infty}^{\infty}\{1-\exp[-n\sigma_0/(1+x^2)]\}dx\right]^2.$$

For $n\sigma_0 < 0.14$, $F(n\sigma_0) = \frac{1}{4}\pi n\sigma_0(1-\frac{1}{2}n\sigma_0)$ to 0.2 percent.
For $n\sigma_0 > 10$, $F(n\sigma_0) = 1-1/2n\sigma_0$ to 0.2 percent.

For an extremely thick sample ($n\sigma_0 \gg 1$) or an extremely thin sample ($n\sigma_0 \ll 1$), the integral for A_E can be evaluated analytically, giving, respectively,

$$A_E^2 = \pi n\sigma_0\Gamma^2 \quad \text{for} \quad n\sigma_0 \gg 1,$$
$$A_E = \tfrac{1}{2}\pi n\sigma_0\Gamma \quad \text{for} \quad n\sigma_0 \ll 1.$$

For intermediate values of $n\sigma_0$, the integral for A_E has

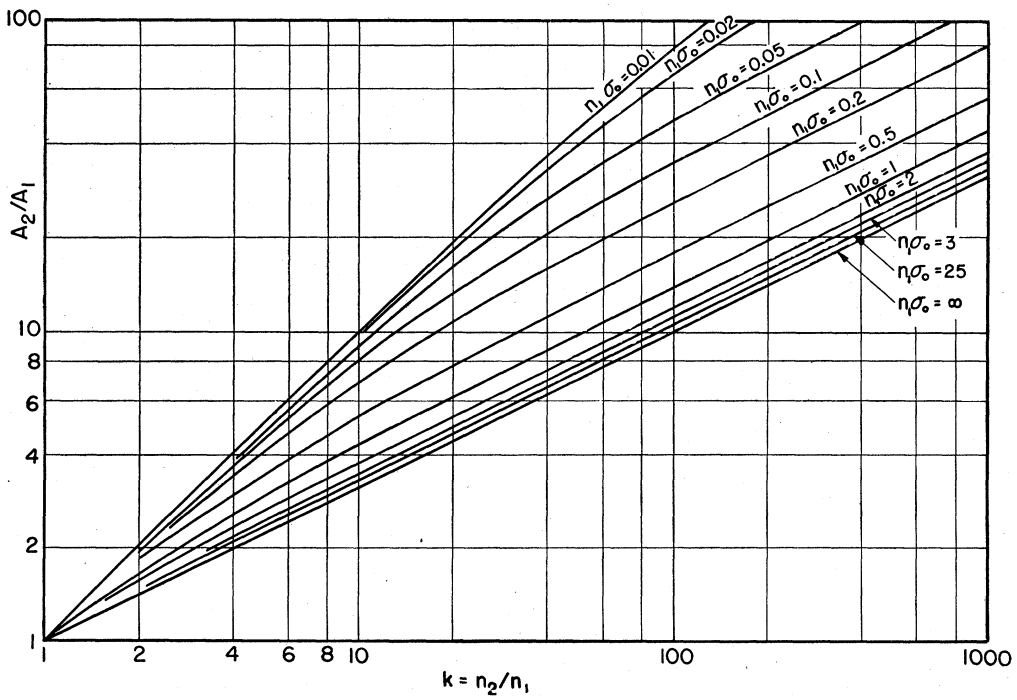

FIG. 2. A_2/A_1 as a function of n_2/n_1 where A = area above transmission dip, n = sample thickness, and the subscripts 1 and 2 refer to thin and thick samples, respectively. With the aid of this graph, σ_0 (and then Γ) for a level may be obtained when measurements on two samples have been made.

been evaluated numerically, and the functions,

$$F(n\sigma_0)=\frac{4E_0^2A_t^2}{\pi n\sigma_0\Gamma^2t_0^2}=\frac{A_E^2}{\pi n\sigma_0\Gamma^2}$$

and

$$G(n\sigma_0)=\frac{4E_0A_t}{\pi n\sigma_0\Gamma t_0}=\frac{2A_E}{\pi n\sigma_0\Gamma},$$

are plotted for the range $0.1\leq n\sigma_0\leq 10$ in Fig. 3 of Paper IV.[2] These functions may also be evaluated by the use of Bessel functions.[5] The function $F(n\sigma_0)$ is of particular significance in the present analysis and is shown in Fig. 1.

If now the expression for $F(n\sigma_0)$ be solved for Γ, we have

$$\Gamma=A_E/[\pi n\sigma_0F(n\sigma_0)]^{\frac{1}{2}},$$

which is an explicit relationship between Γ and σ_0 provided "A_E" and "n" are known. If measurements are available on a second sample of sufficiently different thickness, a second relationship between Γ and σ_0 is obtained. If these relationships are plotted, the intersection of the two curves gives the value of σ_0 and Γ directly.

The simultaneous solution of the two relationships between Γ and σ_0 may be obtained in a somewhat different fashion by eliminating Γ from the two relationships, giving

$$A_2/A_1=[kF(kn_1\sigma_0)/F(n_1\sigma_0)]^{\frac{1}{2}},$$

where $k=n_2/n_1$, and the subscripts 1 and 2 refer to the two samples. Figure 2 shows A_2/A_1 plotted against k for several values of $n_1\sigma_0$. The value of $n_1\sigma_0$ can thus be read off the graph directly when A_2/A_1 and k are known. Γ may then be evaluated in terms of σ_0. The only approximation used in this method of analysis is the assumption of the one level Breit-Wigner formula with the "$1/v$" term and the interference term neglected. These methods are similar to the one suggested in IV,[3] but eliminate the successive approximation feature inherent therein.

The usefulness of the above method of analysis is usually limited by the accuracy of the area determination. The least accurate part of this determination, in many cases, is the determination of the contribution to the area of the "wings" of the curve. The uncertainties arise in part from the presence of other unknown contributions to the cross section, e.g., uncer-

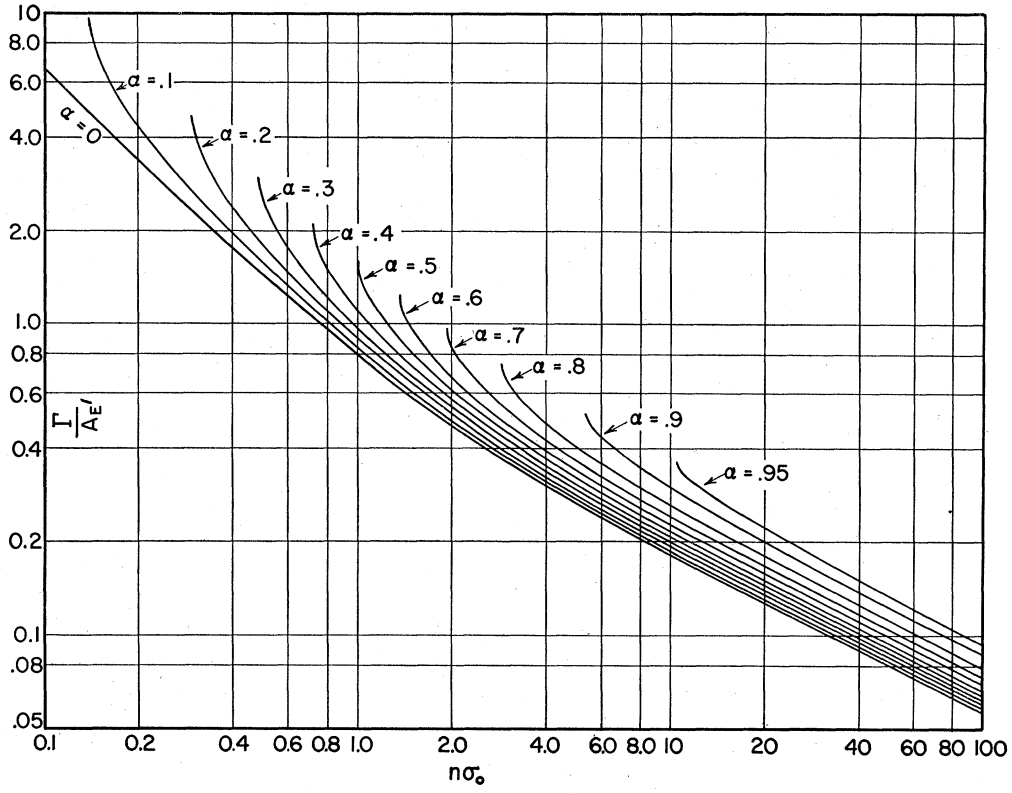

FIG. 3.

$$\frac{\Gamma}{A_E'}=\frac{1}{[\pi n\sigma_0F(n\sigma_0)]^{\frac{1}{2}}}\cdot\frac{2}{1+[1-\alpha/F(n\sigma_0)]^{\frac{1}{2}}}$$

as a function of $n\sigma_0$ and $\alpha=2A_E'/\pi\epsilon$, where $E\pm\epsilon$ are the cut-off points. (When measurements are made on a time-of-flight basis, $A_E'=2(E_0/t_0)A_t'$, and $\alpha=(2A_t'/\pi\tau)$, where $t_0\pm\tau$ are the cut-off points.)

[5] G. V. Dardel and R. Persson, Nature **170**, 1117 (1952).

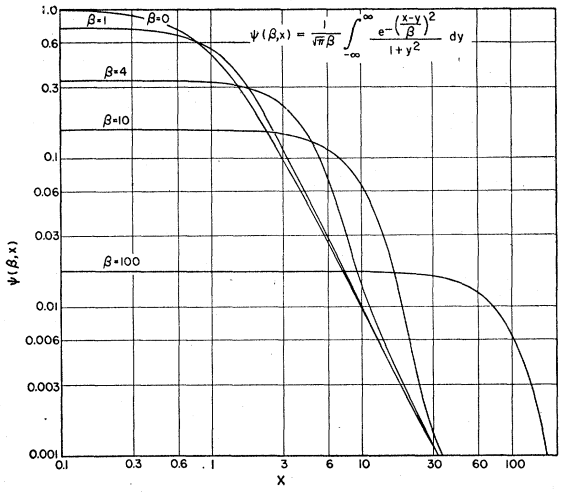

FIG. 4. $\psi(\beta, x)$ as a function of x for several values of β.

tainty in evaluating T_{const} and overlapping of nearby levels from other isotopes and spin states. These difficulties can be minimized by using the following procedure for the treatment of the wing area. First, only the portion of the wings which seems reliable is included in the area to give a partial area A_E' or A_t'. This is used to obtain the first approximate values of σ_0 and Γ. Using these values, the area under the portion of the wings not previously included is calculated and added to the original value to give the next approximation A_E'' or A_t'' and new values of σ_0 and Γ. This process may be repeated until succeeding values do not change.

The successive approximation feature of the method just described can be eliminated in the following manner. Let the wings of the experimental transmission curve be cut off symmetrically about the resonance energy (or time-of-flight) at a point such that T_r is 0.9 or greater. Under these conditions, if the instrumental resolution function does not itself have wings that partially smear the resonance over a wide region, the experimental curves and the actual T_r curves will nearly coincide in the wings. Then the Breit-Wigner relation may be used for T_r beyond the cut-off points. Using only the first term in the expansion of $(1-T)$ in the wing area, the calculated wing area which was omitted is $n\sigma_0\Gamma^2/2\epsilon$, where $E_0\pm\epsilon$ are the energies at which the curve was cut off. Then,

$$(A_E)=(A_E')+n\sigma_0\Gamma^2/2\epsilon.$$

Using the previous expression for A_E, a solution for Γ may be obtained in the following form:

$$\Gamma=\frac{A_E'}{[\pi n\sigma_0 F(n\sigma_0)]^{\frac{1}{2}}}\cdot\frac{2}{1+[1-\alpha/F(n\sigma_0)]^{\frac{1}{2}}},$$

where $\alpha=2A_E'/\pi\epsilon$.

The above expression gives Γ in terms of the measured (partial) area A_E' (i.e., excluding the wings) and the value of σ_0. Then, if two sample thicknesses are used, curves of Γ *vs* σ_0 may be plotted for both samples with the best selection determined from the intersection. To simplify these calculations, a plot of Γ/A_E' *vs* $n\sigma_0$ for various values of α is given in Fig. 3. The case $\alpha=0$ reduces to the earlier problem where the wings have not been cut off.

In many cases, only one sample thickness has been used for the measurement of A_E' with significant precision. If the sample has $n\sigma_0\gg1$ (or $n\sigma_0\ll1$), then $\sigma_0\Gamma^2$ (or $\sigma_0\Gamma$) is determined. For elements having mainly capture at resonance, Γ is usually found to be ~0.1 ev and σ_0 may be estimated assuming $\Gamma=0.1$ ev. If the resulting $n\sigma_0$ is not $\gg1$ (or $\ll1$), a relation of the form $\sigma_0\Gamma^P=M$ gives a more accurate statement of the experimental result than either $\sigma_0\Gamma^2=M'$ or $\sigma_0\Gamma=M''$. The proper choice of P, where $1\leq P\leq2$, is determined from the slope of a plot of $\log\Gamma$ *vs* $\log\sigma_0$ near $\Gamma=0.1$ ev. Values of P and M are given in this report for many of the levels investigated. For $n\sigma_0>3$, it is a fair approximation to use

$$F(n\sigma_0)=1-0.5/n\sigma_0.$$

With this expression for $F(n\sigma_0)$, p and M may be evaluated explicitly, giving

$$P=2\left[1+\frac{\pi}{8}\frac{[1+(1-\alpha)^{\frac{1}{2}}]^2}{(1-\alpha)^{\frac{1}{2}}}\frac{\Gamma^2}{A_E'^2}\right]^{-1},$$

$$M=\frac{1}{n}\{(4A_E'^2/\pi)[1+(1-\alpha)^{\frac{1}{2}}]^{-2}+\Gamma^2[2(1-\alpha)^{\frac{1}{2}}]^{-1}\}\times\exp[(2-p)\ln(1/\Gamma)].$$

The quantities are to be evaluated at a value of Γ,

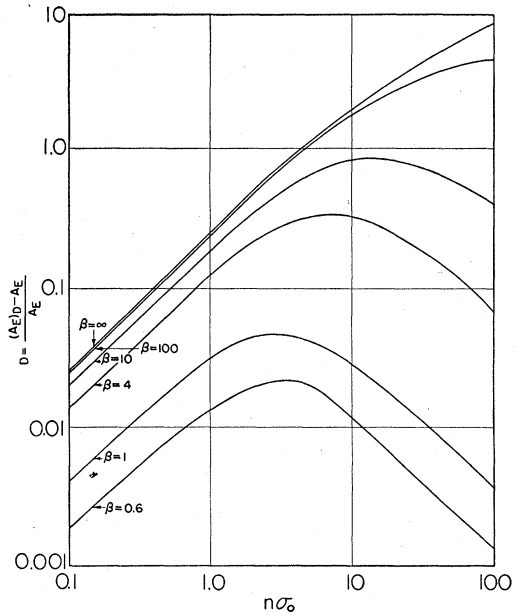

FIG. 5. Effect of Doppler broadening upon area above transmission dip. (D as a function of $n\sigma_0$ for various values of β.)

generally 0.1 ev, in the neighborhood of which these relationships are to hold.

Evaluation of the Doppler Effect

In the previous analysis, the thermal motion of the nucleus has been neglected. If the width of the level, Γ, is large compared to the Doppler width, the previous analysis can be applied directly. However, if this is not the case, then the cross section near resonance is no longer given by the one-level Breit-Wigner formula. Instead, this formula must be averaged over the thermal motion of the nucleus.[6] The area above the transmission dip will now be larger than that obtained when the Doppler width is neglected.

When the Doppler effect is included, the area above the transmission curve is given by the formula

$$[A_E]_D=\tfrac{1}{2}\Gamma\int_{-\infty}^{\infty}[1-\exp\{-n\sigma_0\psi(\beta, x)\}]dx,$$

where

$$x=2(E-E_0)/\Gamma,\quad \beta=2\Delta/\Gamma,\quad \Delta=(4mEkT/M)^{\frac{1}{2}},$$

and

$$\psi(\beta, x)=\frac{1}{\pi^{\frac{1}{2}}\beta}\int_{-\infty}^{\infty}\frac{1}{1+y^2}\exp\left\{-\frac{(x-y)^2}{\beta^2}\right\}dy,$$

where $y=2(E'-E_0)/\Gamma$ and E' is the energy of the neutron relative to the nucleus. These integrations probably cannot be carried out analytically and one must resort to the use of series expansions and numerical methods. $\psi(\beta, x)$ may always be calculated from the

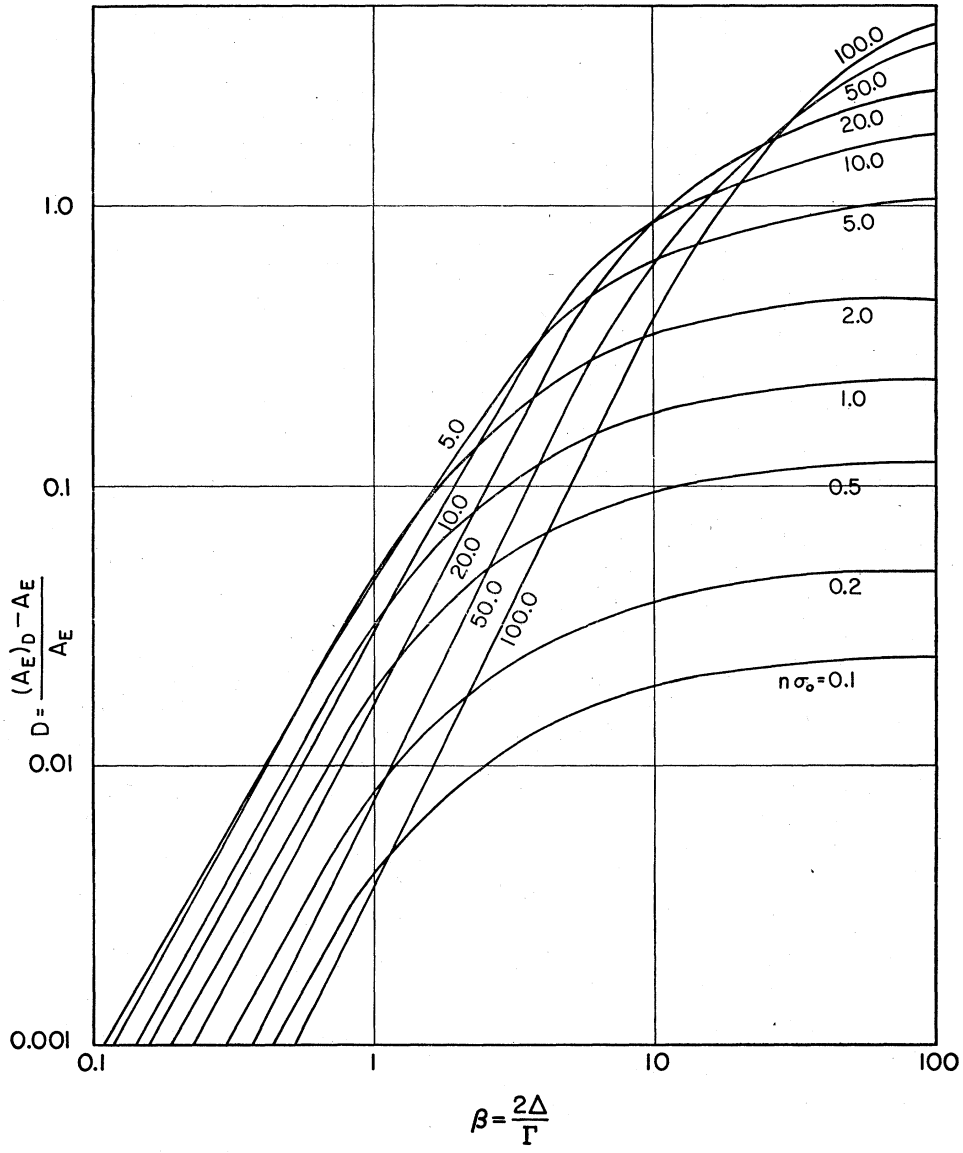

FIG. 6. Effect of Doppler broadening upon area above transmission dip. (D as a function of β for several values of $n\sigma_0$.)

[6] H. A. Bethe, Revs. Modern Phys. **9**, 67 (1937).

convergent series:

$$\psi(\beta, x)=\exp(-x^2/\beta^2)\left\{I_0+\frac{1}{2!}\left(\frac{2x}{\beta^2}\right)^2 I_1 + \frac{1}{4!}\left(\frac{2x}{\beta^2}\right)^4 I_2+\cdots+\frac{1}{(2n)!}\left(\frac{2x}{\beta^2}\right)^{2n} I_n+\cdots\right\},$$

where

$$I_0=(\pi^{\frac{1}{2}}/\beta)\exp(1/\beta^2)[1-\varphi(1/\beta)],$$

$$I_1=1-I_0,$$

$$I_{n+1}=\frac{1\cdot 3\cdot 5\cdots(2n-1)}{2^n}\beta^{2n}-I_n \text{ for } n\geq 1,$$

$$\varphi(1/\beta)=\frac{2}{\sqrt{\pi}}\int_0^{1/\beta}\exp(-t^2)dt.$$

However, this series converges too slowly unless $2x/\beta^2$ is small. For large values of x and/or small values of β_1 the semiconvergent series,

$$\psi(\beta, x)=\frac{1}{1+x^2}\left\{1+\frac{\beta^2}{2}\frac{3x^2-1}{(1+x^2)^2}+\frac{3\beta^4}{4}\frac{5x^4-10x^2+1}{(1+x^2)^4} + \frac{15\beta^6}{8}\frac{7x^6-35x^4+21x^2-1}{(1+x^2)^6} + \frac{105\beta^8}{16}\frac{9x^8-84x^6+126x^4-36x^2+1}{(1+x^2)^8}+\cdots\right\},$$

is convenient, but must be used with caution. The series for $[A_E]_D$,

$$[A_E]_D=\tfrac{1}{2}\Gamma\left\{\pi n\sigma_0-\tfrac{1}{2}(n\sigma_0)^2\int_{-\infty}^{\infty}\psi^2(\beta, x)dx + \tfrac{1}{6}(n\sigma_0)^3\int_{-\infty}^{\infty}\psi^3(\beta, x)dx-\cdots + (-1)^n\frac{1}{n!}(n\sigma_0)^n\int_{-\infty}^{\infty}\psi^n(\beta, x)dx+\cdots\right\},$$

is convergent, but the integrals

$$\int_{-\infty}^{\infty}\psi^n(\beta, x)dx$$

usually have to be evaluated numerically.

$\psi(\beta, x)$ for several values of β is shown in Fig. 4. The quantity

$$D=([A_E]_D-A_E)/A_E$$

gives the relative increase in area arising from the Doppler effect. This quantity is shown in Figs. (5) and (6) plotted in two different ways. For the limiting case of $\beta\to\infty$,

$$D\to\{(\pi n\sigma_0/2A_E)-1\}.$$

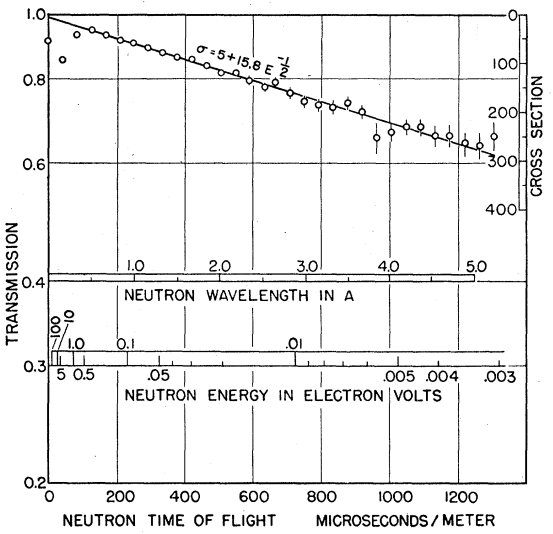

FIG. 7. Slow neutron transmission of 0.518 g/cm² of rhenium in the region below 1 ev showing the "1/v" absorption slope.

One can readily understand the qualitative behavior of the Doppler correction, $D=([A_E]_D-A_E)/A_E$, for the limiting cases of a very thin and a very thick sample for given β. If the sample is very thin ($n\sigma_0\ll 1$), the exponential can be expanded, and in the first approximation, we obtain

$$[A_E]_{D\text{ thin}}=\tfrac{1}{2}\Gamma\int_{-\infty}^{\infty}n\sigma_0\psi(\beta, x)dx,$$

which equals $\frac{1}{2}\pi n\sigma_0\Gamma$ and is exactly the same expression we would obtain if the Doppler effect were not present. Thus, D becomes zero for a very thin sample. If the sample is extremely thick ($n\sigma_0\gg 1$), the transmission of the sample will be effectively zero several level widths away from the center of the level, where the Doppler effect makes the greatest difference in cross section. Further out, when the transmission rises above zero, the Breit-Wigner formula is only slightly affected by the Doppler broadening, so that the area above the transmission curve is only slightly increased. For a given β, these effects become less and less as $n\sigma_0$ becomes greater, and the Doppler correction D approaches zero, in the limit.

Part of this numerical integration has been presented by Dandel and Pressen in a different manner.[5] In our notation, they have presented the region from $\beta=0$ to $\beta=1.2$ for $n\sigma_0$ from 0.2 to 10. However, for high values of $\beta\sim 1$ or greater, the semiconvergent series they used to evaluate their $[A_E]_D$ may not be a good approximation. Some useful expansions, and some values of $\psi(\beta, x)$ over a small range of values of β and x are given in Born's "Optik" (1943) 483 ff.

Summarizing, the application of the Doppler effect to the analysis is as follows. A_E' and α are determined and, for a selected value of $n\sigma_0$, Γ is calculated as usual. This is a first approximation result omitting the Doppler effect. The ratio $\beta=2\Delta/\Gamma$ is calculated and the quantity

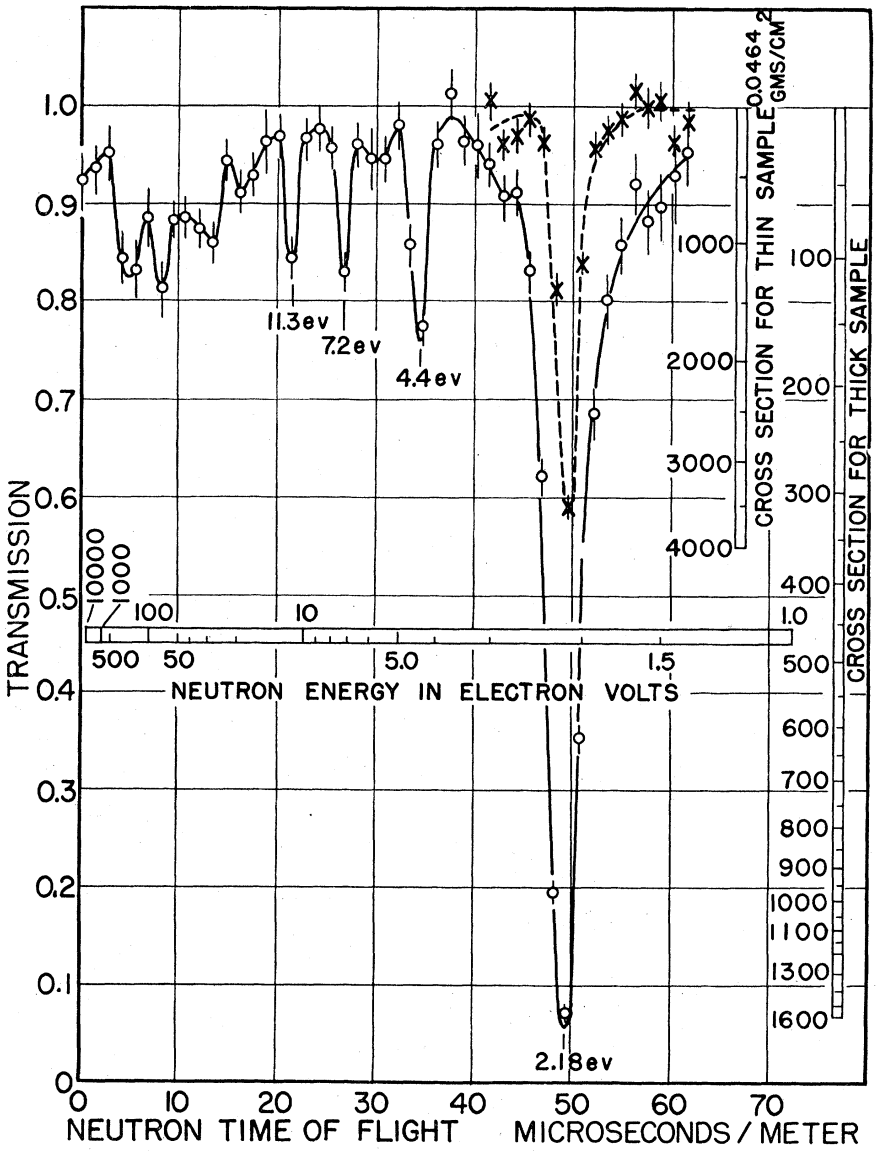

FIG. 8. Slow neutron transmission of 0.518-g/cm² and 0.0464-g/cm² Re with about 3.5-μsec/m resolution.

D read from Fig. (6), which is the more useful of the two plots for this purpose. New values for A_E' and α, are calculated by dividing the initial values by $(1+D)$. For the same $n\sigma_0$, a new Γ is calculated using the new values of A_E' and α. A new value for β is calculated, giving new values of A_E' and α. This successive approximation procedure is continued until the values for Γ do not change. As before, Γ is calculated for various values of $n\sigma_0$, giving the relationship between σ_0 and Γ, but now with the Doppler effect taken into account.

This treatment of the Doppler effect is valid only if the nucleus under consideration is in a gas or is weakly bound in a solid, so that its behavior is as in a gas of some temperature (not necessarily ambient temperature). Under strong binding, the Doppler effect may also shift the position of the level.[7]

[7] W. E. Lamb, Phys. Rev. **55**, 190 (1939).

RESULTS

Rhenium

The slow neutron transmission of rhenium has been investigated using samples of metallic rhenium. A 0.518-g/cm² sample was used throughout the entire energy interval covered. An additional sample of 0.0464 g/cm² was used in the neighborhood of the 2.18-ev level.

Figure 7 shows the measurements in the thermal region. The curve which best fits these data is

$$\sigma=5.0+15.8E^{-\frac{1}{2}},$$

where σ is in barns and E in ev.

The resonance region, studied with better resolution, is shown in Fig. (8) and the higher energy portion, studied with still better resolution, is shown in Fig. (9).

The data in the neighborhood of the 2.18-ev level

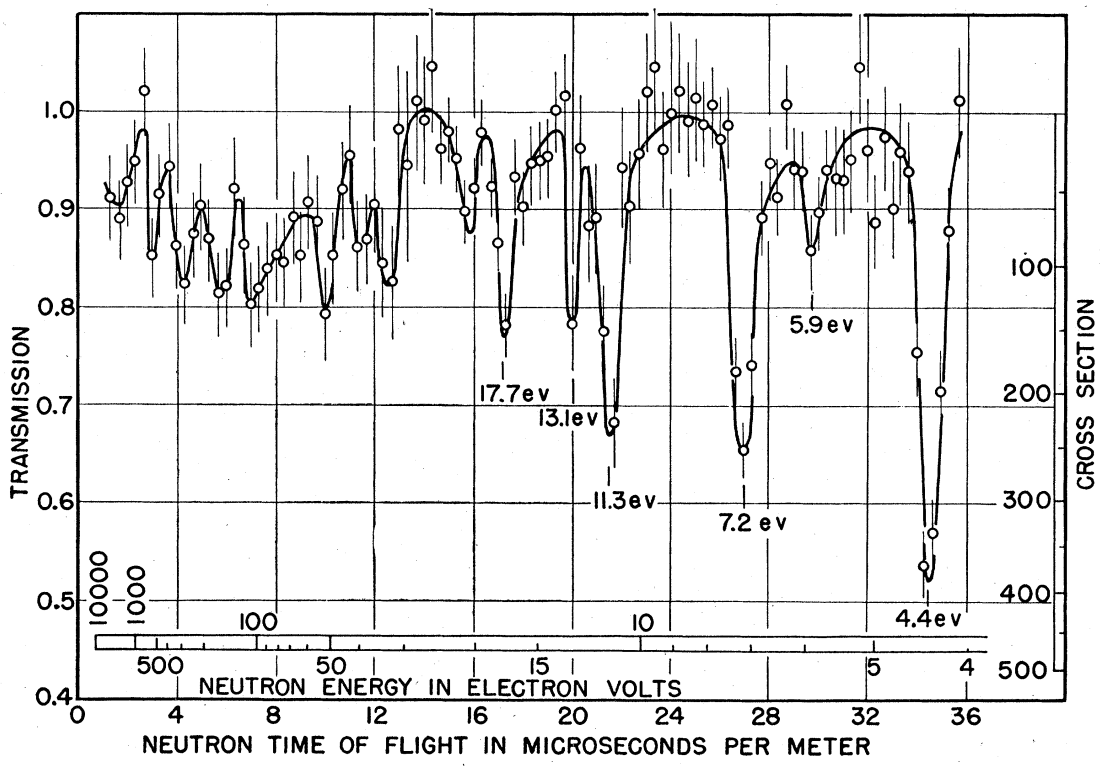

FIG. 9. The slow neutron transmission of 0.518-g/cm² Re with about 1.3-μsec/m resolution.

are suitable for two kinds of analysis: (1) measurement of area above the transmission curve of each of the two samples of different thickness, and determination of σ_0 and Γ from these measurements by the method described earlier in this report, and (2) curve fitting in which the resolution function is applied to successive theoretical curves until a best fit is obtained.

In applying the area method, the transmission was plotted against energy. The areas were determined to chosen values of the energy symmetrically placed on each side of the resonance energy. (For the "thin" sample, this cut-off energy was 0.40 ev from resonance, and for the "thick" sample 0.70 ev.) These values were chosen such that the transmission was greater than 0.90 so that there was very little resolution smearing beyond cutoff. The two curves of σ_0 *vs* Γ are shown in Fig. 10 and the intersection of the two curves gives the following values:

$$\sigma_0 = 5700 \text{ barns}, \quad \Gamma = 0.090 \text{ ev},$$

from which

$$\sigma_0\Gamma = 513 \text{ barn ev}, \quad \sigma_0\Gamma^2 = 46.2 \text{ barn ev}^2.$$

It is interesting to note that $n\sigma_0$ for the "thin" sample is 0.85, so that the thin sample approximation is in error by 17 percent (Fig. 3 of paper IV).[2]

The method of curve fitting has also been applied to this level. This method is particularly useful when data on only one sample thickness are available. In the case of the Re 2.18-ev level, application of both methods gives a check on the consistency of the data and the methods. Since an area measurement above the transmission dip gives a relationship between σ_0 and Γ, only one of these need be varied in seeking the best fit to the data. Figure 11 gives an enlarged plot of the thick sample data on the 2.18-ev level. The calculated transmission curves are based on a value of $\sigma_0\Gamma^2 = 46.2$ (which can be obtained by measurement on the thick sample alone), and three values of Γ: 0.070, 0.090, and 0.120 ev. The broadening arising from the Doppler effect was first applied to the calculated cross

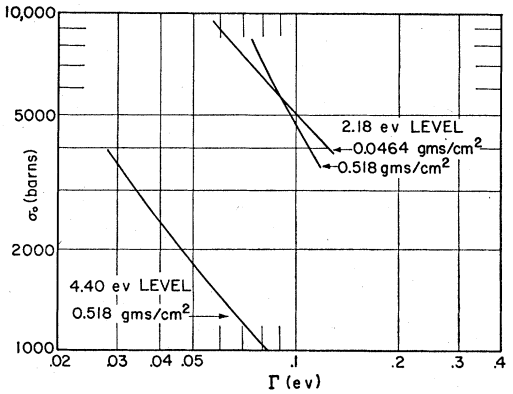

FIG. 10. A plot of σ_0 *vs* Γ for the 2.18-ev level of Re using two sample thicknesses and the 4.40-ev level of Re using one sample thickness.

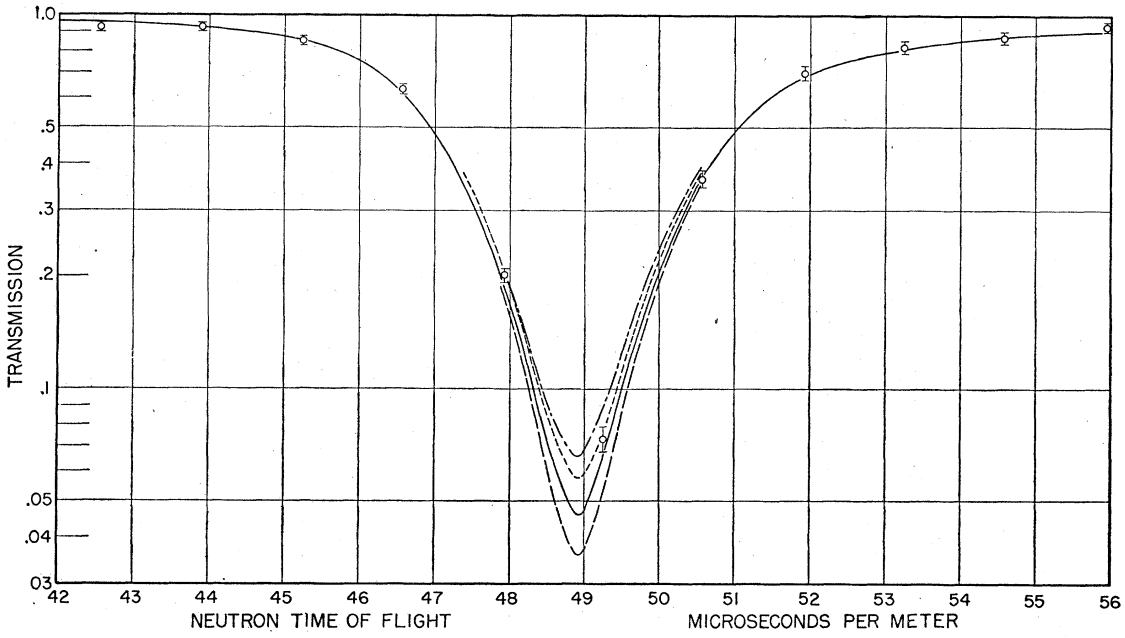

FIG. 11. Curve fits for the 2.18-ev level of Re with $\sigma_0\Gamma^2=46.2$. In the ——— curve, $\Gamma=0.09$, which is the best value from the area method; in the — — — curve, $\Gamma=0.07$; in the — — — — curve, $\Gamma=0.012$; the - - - - curve is for $\Gamma=0.09$ without the Doppler correction.

section for each value of Γ, the same type of correction being assumed as for Re gas at room temperature. The transmission was then calculated and the resolution function applied to each curve. The resolution function was taken as a triangle of base 3.5 μsec/m which takes into account the arc pulse width (8 μsec), the detection width (8 μsec), and a broadening of 1.7 percent of the time of flight arising from the finite length (10 cm) of the BF_3 counter used. The resulting curves are shown in Fig. 11. The curve with $\Gamma=0.090$ ev gives a much better fit to the data, as expected from the results of the previous method of analysis. The transmission curve for $\Gamma=0.090$ ev, but without the Doppler broadening, is also included in Fig. 11, showing a difference equivalent to about 0.02 ev in Γ. This curve seems to fit the lowest transmission point better than the curve with the Doppler correction. However, for this level, the resolution width is almost twice the level width so that the curve fitting method is very sensitive to the choice of the shape and width of the resolution function.

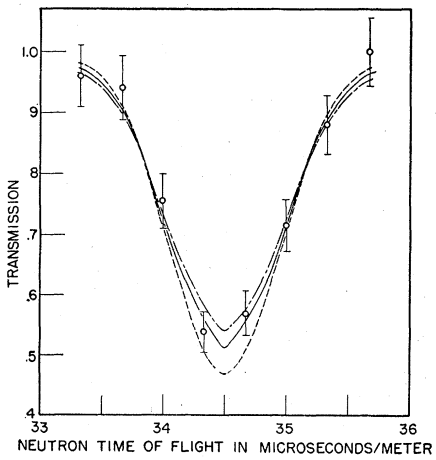

FIG. 12. The curve fit for the 4.40-ev level in Re. For each value of Γ, the value of σ_0 obtained from Fig. 10 is used. The — — — — curve is for $\sigma_0=1300$ barns, $\Gamma=0.07$ ev; The ——— curve is for $\sigma_0=2000$ barns, $\Gamma=0.05$ ev; The - - - - curve is for $\sigma_0=4000$ barns, $\Gamma=0.03$ ev.

Since σ_0 and Γ are known, Γ_n can be calculated from the formula $\Gamma_n=\sigma_0\Gamma/4\pi\lambda\!\!\!^{-2}f$, provided f is known. Now $f=\frac{1}{2}a[1\pm(2i+1)^{-1}]$, where a is the isotopic abundance and i the nuclear spin of the responsible isotope. Re has two stable isotopes, 37.1 percent of the $A=185$ isotope, and 62.9 percent of the $A=187$ isotope. The spins of both isotopes are 5/2. Measurements in the separated Re isotopes show that the 2.18-ev level is in the $A=185$ isotope,[8] so that $f=0.159$ or 0.223. Since the responsible

TABLE I. Parameters for the first eight levels in Re.

t_0 (μsec/m)	E_0 (ev)	P	M	σ_0(barns) for $\Gamma=0.1$ ev	$\Gamma_n E_0^{-\frac{1}{2}}$ $=\frac{\sigma_0\Gamma E_0^{\frac{1}{2}}\,a}{2.62\times10^6 f}$	$\frac{\sigma_0\Gamma^2}{4E_0^{\frac{1}{2}}}$	Isotopic assignment
49.0	2.18				15×10^{-4}	3.59	Re^{185}
34.5	4.40				3×10^{-4}	0.14	Re^{187}
29.7	5.92	1.00	26	260	1×10^{-4}	0.05	
27.0	7.18	1.41	43	1100	4×10^{-4}	0.14	
21.5	11.3	1.74	48	2600	13×10^{-4}	0.17	Re^{187}
20.0	13.1	1.60	48	1900	10×10^{-4}	0.10	
17.2	17.7	1.85	60	4200	27×10^{-4}	0.15	
15.8	21.1	1.73	35	1900	13×10^{-4}	0.05	
						4.4 (sum)	

[a] f taken as $\frac{1}{4}$ except when other values are given in the text.

[8] Argonne National Laboratory, Quarterly Report, March–May 1951, Physics Division (unpublished).

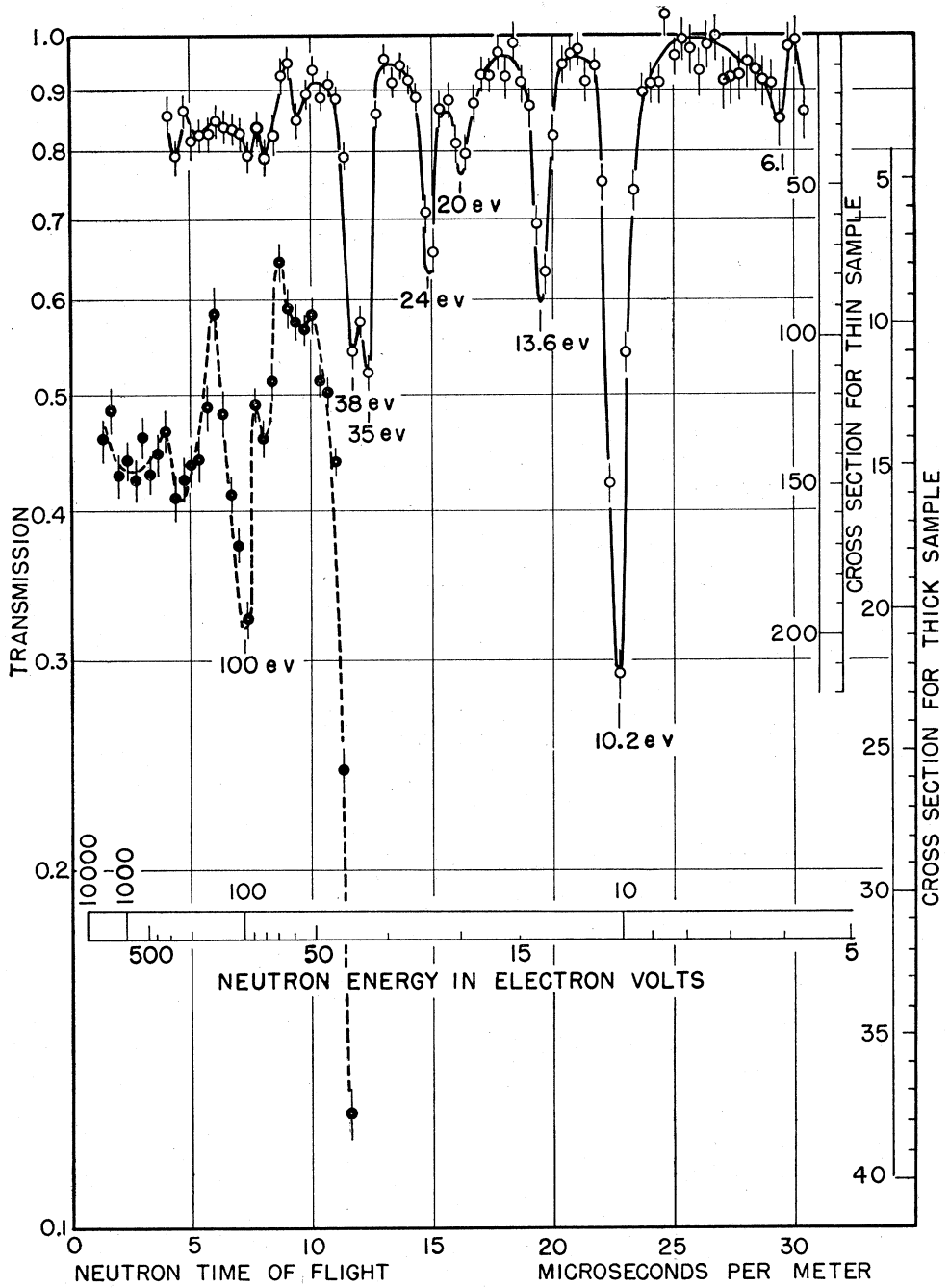

FIG. 13. The slow neutron transmission of 1.73 g/cm² (○) and 16.54 g/cm² (●) of Ta.

spin state is not known, an average value $f=0.19$, is used. This gives $\Gamma_n=0.0022$ ev.

Also,

$$\sigma_{0s}/\sigma_{0c}=\Gamma_n/\Gamma_\gamma=\Gamma_n/(\Gamma-\Gamma_n)=0.025,$$

so that this level has 97.5 percent capture and 2.5 percent scattering. The quantity $\Gamma_n E_0^{-\frac{1}{2}}=0.0015$.

The method of curve fitting has also been applied to the 4.40-ev level, for which data were taken on only one sample. An area measurement leads to the relationship between σ_0 and Γ which is shown in Fig. 10. Figure 12 shows an enlarged plot of this level with curves for three pairs of values of σ_0 and Γ from Fig. 10. The Doppler effect has been taken into account. The best values are seen to be $\sigma_0=2000$ barns, $\Gamma=0.05$ ev. However, uncertainties in the data and in the choice of resolution functions make for large possible errors in the values of σ_0 and Γ. This level is in Re^{187},[8] so that $\Gamma_n=0.00054$ ev (taking $f=0.31$).

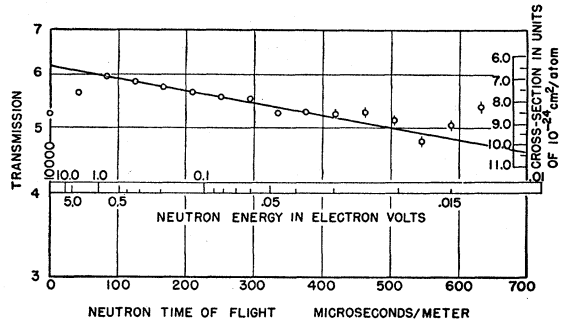

FIG. 14. The slow neutron transmission of 12.67 g/cm² of Ru with broad resolution. Below 1 ev the data are well fitted by $\sigma=6.4+0.39E^{-\frac{1}{2}}$ until crystal interference effects begin.

For the levels at higher energies, measurements on only one sample are available. (A second, thinner sample would probably not be of much use unless the levels were much better resolved.) To get as much information as possible, area measurements were made on those levels which appeared reasonably well resolved as single levels. In measuring an area, a triangular approximation for the form of the transmission curve was assumed, since for resolution width large compared with Γ, as is the case here, the transmission curve outlines the shape of the resolution function rather than the shape of the level. Using the method described, which takes into account the "wing" area missed by the triangular approximation, the values of P and M in

$$\sigma_0\Gamma^P=M$$

were calculated and are listed in Table I. Values of σ_0 for $\Gamma=0.1$ ev are also given. Since the results on the higher energy levels are exceedingly rough, the Doppler effect has not been taken into account.

Each of these levels contributes to the thermal $E^{-\frac{1}{2}}$ slope the amount

$$\sigma_0\Gamma^2/4E_0^{\frac{3}{2}}.$$

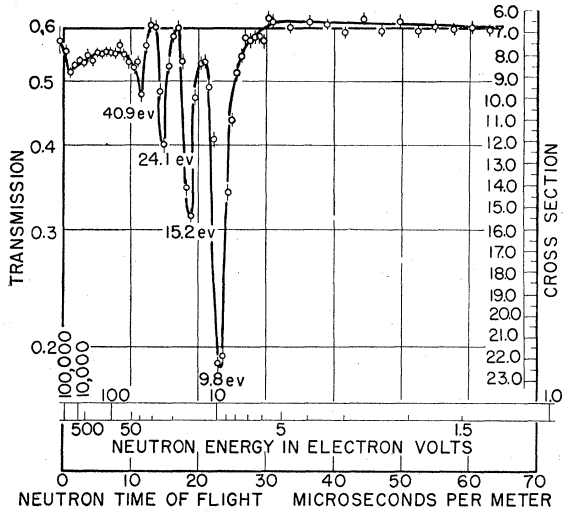

FIG. 15. The slow neutron transmission of 12.67 g/cm² of Ru with a resolution of 1.3 μsec/m (full width at base of triangle).

The sum of these contributions is seen to be 4.4 from Table I.

The measurement in the thermal region gives a value of 15.8 for the slope, indicating contributions from levels other than those considered. These may come from levels higher in energy and from negative levels close to zero. If the entire effect is due to a single negative level at -1 ev, it must have $\sigma_0\Gamma^2=44$ which is in line with $\sigma_0\Gamma^2$ for the other levels. Also, a separation of 3 ev from the 2.18-ev level is reasonable considering the close spacing of the higher levels.

Tantalum

Tantalum has been reinvestigated in the energy range from 40–5000 ev with a sample containing 16.54 g/cm², and in the energy range from 5–300 ev with a sample containing 1.73 g/cm². A spectrographic analysis of the sample showed lines of Fe, Ni, Cb, Si, Cu, Mg, Ca, and Mn. Concentration of all the impurities were estimated to be 0.01 percent or less. In both cases, the arc width was 4 μsec and the detection width was 2 μsec, with the base of resolution triangle being about 1.4 μsec/m (including the broadening arising from the length of the counter). Results of these measurements are shown in Fig. 13. There is considerably more detail observed in this transmission curve than shown in a previously published one by Havens *et al.*[2] In particular, the level at 22 ev has been resolved into two levels at 20 and 24 ev and the level at 37 ev has been resolved into levels at 35 and 38 ev. There are other pronounced dips at higher energies. However, because of the closeness of level spacing, it is impossible to obtain any information about the level structure above 50 ev.

TABLE II. Parameters for some of the levels in Ta.

t_0 (μsec/m)	E_0 (ev)	$\sigma_0\Gamma^2$ (barn ev²)	P	M	$\Gamma_n E_0^{-\frac{1}{2}}$ (ev$^{\frac{1}{2}}$)	$\sigma_0\Gamma^2/4E_0^{\frac{3}{2}}$ (barn ev$^{\frac{1}{2}}$)
11.7	38.2	280	1.99	280	0.013	0.297
12.2	35.1	200	1.99	200	0.009	0.235
14.8	24.0	39	1.95	44	0.0015	0.083
16.2	20.0	10.3	1.80	16.0	0.0002	0.029
19.5	13.7	11	1.80	17.0	0.0002	0.054
22.6	10.2	48	1.96	54	0.0012	0.372
29.2	6.1	···	0.91	5.4	0.000008	0.009
					Sum:	1.08

The levels between 5 and 50 ev are listed in Table II. For all but the 6.1-ev level, the thick sample approximation is fairly reliable and values of $\sigma_0\Gamma^2$ are included. More generally, the values of the parameter 'P' and 'M' are given for $\sigma_0\Gamma^P=M$. It is expected that P should be between 1 and 2 and at first glance, it seems surprising to find it 0.91 for the case of the 6.1-ev level. This can be accounted for in the following way: the level shape is approximated by a triangle plus an amount for the 'wings' of the Breit-Wigner curve. The amount added depends upon the value of Γ assumed, and since the contribution of the wings is quite large for this level (about 15 percent if $\Gamma=0.1$ ev), the varia-

tion of the amount added is enough to affect the value of P appreciably and depresses it below what should be its lower limit. It is possible that this level is in an impurity, or even that it is spurious because of the large statistical uncertainty.

Table II also shows values for $\Gamma_n E_0^{-\frac{1}{2}}$, calculated taking $\Gamma=0.1$ ev when necessary and $\frac{1}{2}$ (average value) for the statistical weight factor. One might expect two distinct values, one for each spin state (Tantalum is monoisotopic.) However, no such grouping is observed.

Table II includes values of the quantity $(\sigma_0\Gamma^2)/(4E_0^{\frac{3}{2}})$. This is the contribution of each level to the $1/\sqrt{E}$ slope in the thermal region. The sum for these levels is 1.08. Recalculation for the case of the 4.1-ev level discussed in the previous report gives $\sigma_0\Gamma^2=55.4$, from which $(\sigma_0\Gamma^2)/(4E_0^{\frac{3}{2}})=1.67$, making a total of 2.75. The measured thermal $1/\sqrt{E}$ slope is 3.0. The difference is small and may be due to errors in calculating the quantities involved in the comparison, contributions from levels higher up in energy, and contributions from negative energy levels.

Ruthenium

Transmission curves are shown in Figs. 14 and 15 for a sample containing 12.67 g/cm². A spectrographic analysis of the sample showed no impurity lines. A trace mixture of other elements was then added to the sample. These trace elements were then observed to the degree expected. This analysis showed the Ruthenium to be extremely pure.

TABLE III. Parameters for the first four levels in Ru.

t_0 (μsec/m)	E_0 (ev)	$\sigma_0\Gamma^2$ (barn ev²)	$\sigma_0\Gamma^2/4E_0^{\frac{3}{2}}$ (barn ev$^{\frac{1}{2}}$)
11.3	40.9	32.0	0.031
14.7	24.1	18.0	0.038
18.6	15.2	14	0.061
23.1	9.8	15	0.125
		Sum:	0.255

Figure 14 shows the energy interval 0.01 ev to 10 ev taken with broad resolution. In the energy interval just above where crystal interference effects become important, the cross section is well matched by the curve $\sigma=6.4+0.39E^{-\frac{1}{2}}$.

Figure 15 shows the energy interval from 1 ev to 1000 ev with a resolution of about 1.3 μsec/m (full width at base). There are strong dips in transmission at 23.1, 18.6, 14.7, and 11.3 μsec/m. Each of these dips was assumed to be caused by a single resonance level. For all of these levels, the sample was found to be decidedly thick (i.e., $n\sigma_0\gg1$) so that Table III lists values of $\sigma_0\Gamma^2$.

Ruthenium has 7 isotopes ranging from $A=96$ to $A=104$, with concentrations ranging from 2.2 percent to 31.3 percent. No assignment of the levels to particular isotopes can be made with the normal sample used.

The four levels listed contribute $0.26E^{-\frac{1}{2}}$ to the thermal region, leaving $0.13E^{-\frac{1}{2}}$ to be made up by errors, higher energy levels, and negative levels. (With the observed spacing of levels, a nearby negative level is likely.)

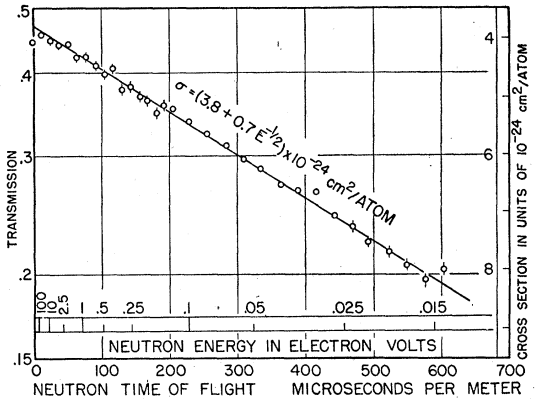

FIG. 16. The slow neutron transmission of 17.2 g/cm² of Cr taken with broad resolution. The data are well-fitted by $\sigma=3.8+0.7E^{-\frac{1}{2}}$.

Chromium

A 17.2 g/cm² sample was used in all of these measurements. A spectrographic analysis of the sample showed ~0.1–1 percent Mn, ~0.1 percent Fe and Si, and 0.01 percent or less of Al, Ca, Cb, Cu, Mg, Mo, Ni, Ti, and V. Further analysis showed Mn and W to be present to 0.2 percent. The thermal region shown in Fig. 16 is well-matched by

$$\sigma=3.8+0.7E^{-\frac{1}{2}}.$$

Figure 17 shows the region above 3 ev taken with moderate resolution. Calculation of $\sigma_0\Gamma^2$ from the data of Fig. 17 for the known tungsten impurity of 0.2 percent, showed that the 18-ev level was due to tungsten. The dip at 12 ev did not repeat consistently in several runs and is probably spurious.

The level evident at higher energies, and shown with much better resolution in Fig. 18 to be at 3800 ev, has also been analyzed by the area method, giving $\sigma_0\Gamma^2=8.55\times10^7$ barn ev². If this is assumed to be a scattering level in the predominant isotope ($A=52$, 83.3 per-

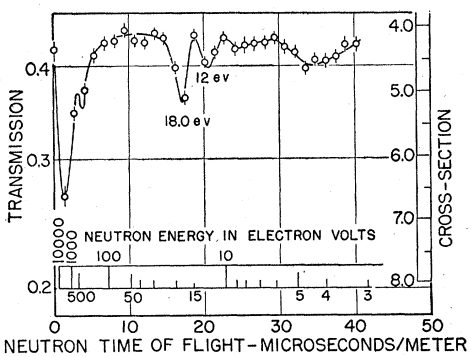

FIG. 17. The slow neutron transmission of 17.2 g/cm² of Cr taken with a resolution of 3.0 μsec/m (full width at base of triangle).

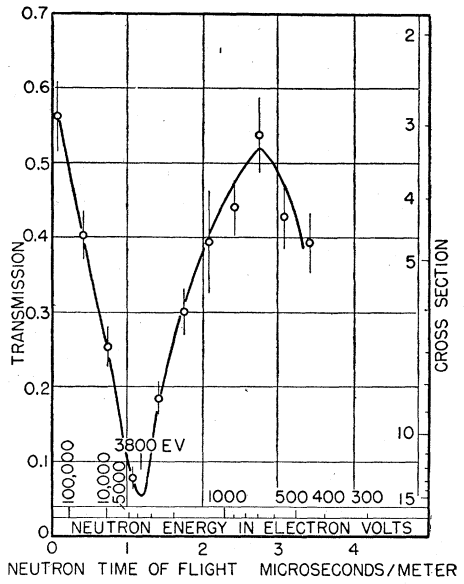

FIG. 18. The slow neutron transmission of 17.2 g/cm² of Cr taken with a resolution of 1.1 μsec/m (full width at base of triangle) showing the large level at 3800 ev.

cent) the maximum cross section is 690 barns for the isotope (taking spin=0), giving $\Gamma=385$ ev. If the thermal absorption is attributed to a small amount of capture in this level, calculation gives $\Gamma_\gamma/\Gamma=0.0076$, showing that only 0.76 percent of the neutrons forming the compound nucleus leads to a new isotope.

If the assignment of the 3800-ev level to the predominant isotope is correct, it is expected that the shape of the transmission curve at lower energies would be different from what it is. Calculations indicate that the interference minimum in cross section should be at about 1000 ev and very small (<1 percent) compared with $4\pi R^2=3.95$ barns. Recovery to this value at lower energies should also be very slow. There is no definite way to resolve this situation without further measure-

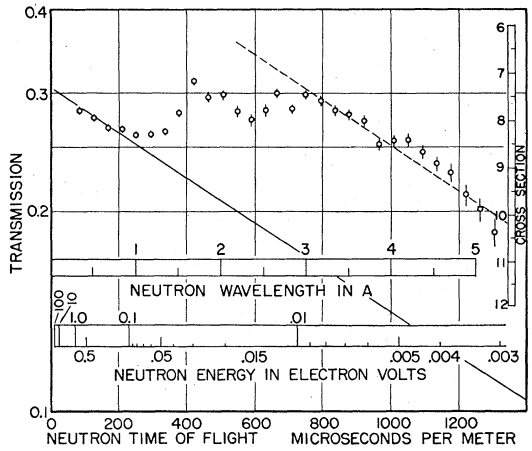

FIG. 19. The slow neutron transmission of 18.74 g/cm² of Ga in the thermal region showing interference effects. ——— represents $\sigma=7.3+0.35E^{-\frac{1}{2}}$; — — — represents $\sigma=3.6+0.35E^{-\frac{1}{2}}$.

TABLE IV. Abundance and absorption cross sections of the Cr isotopes.

Isotope	Percent abundance	σ_{abs} at 0.025 ev, in barns
Cr^{50}	4.4	16.3 ±1.3
Cr^{52}	83.7	0.73±0.06
Cr^{53}	9.5	17.5 ±1.4
Cr^{54}	2.4	<0.3

ments. It is possible that the level is due to one of the other isotopes, say $A=53$, which is 9.43 percent abundant. Then, $\sigma_0\Gamma^2$ is increased to 1.81×10^9 for the isotope and spin state and Γ becomes 1620 ev. (The spin of the $A=53$ isotope is unknown, and only its average effect has been taken into account in this calculation.) If one of the rarer isotopes is actually responsible for this level, the low energy behavior of the cross section (<1000 ev) is reasonable since it is dominated by the constant cross section of the predominant isotope and hence approximately constant at about $4\pi R^2$. This explanation is also reasonable in the light of the data given in Table IV, taken from AECU-2040,[4] which shows that capture in the thermal region is due primarily to the two isotopes Cr^{50} and Cr^{53}.

Figure 17 indicates, and other measurements show, that there is a transmission dip in this sample at 4 μsec/m. A portion of this dip is evident in Fig. 18. This dip is due to the 300-ev level in the 0.2 percent Mn impurity in the sample. The 3000-ev level in the Mn impurity is masked by the 3800-ev level in the Cr.

Gallium

An 18.74-g/cm² sample was used in all the investigations. The thermal region is shown in Fig. 19. Crystal interference effects are observed, although not as pronounced as in the case of some other crystals. Ga has a melting point of 29.8°C (=85.6°F), and since the thermal data were taken during summer, the sample was probably liquid part of the time. The interference effects may be due to the sample being solid part of the time. However, liquids are also known to exhibit interference effects as a result of short range order (e.g., liquid bismuth and vitreous quartz). This curve is not useful for determining the $E^{-\frac{1}{2}}$ slope.

Figure 20 shows the 0.05-ev to 5-ev region where a straight line matches the data well, giving $\sigma=7.3+0.35E^{-\frac{1}{2}}$. This equation is shown plotted on the graph of the thermal region. The situation is now clear. With decreasing energy, there are two competing effects: (1) a tendency towards transparency as the number of ways of removing neutrons from the beam (by Bragg reflection) decreases, and (2) an increase in cross section arising from a "$1/v$" capture term. At low energies, the experimental data indicate a straight line of approximately the same slope as the capture term. If the sample were a crystal, one would interpret the difference between the free cross section (7.3 barns) and the difference between the lowest energy data and the line

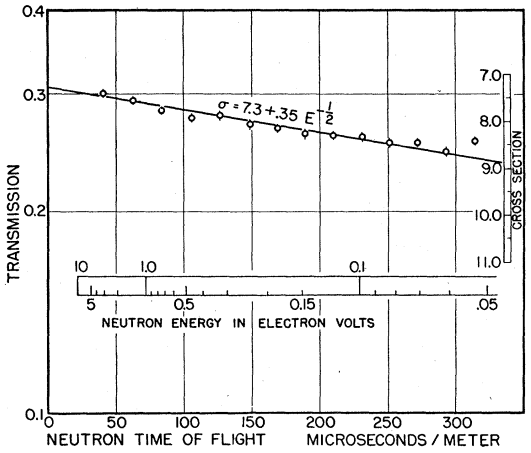

FIG. 20. The slow neutron transmission of 18.74 g/cm² of Ga between 0.05 and 5 ev. The data are well-fitted by $\sigma=7.3+0.35E^{-\frac{1}{2}}$.

$\sigma=7.3+0.35E^{-\frac{1}{2}}$ (3.6 barns) as the incoherent scattering cross section, giving about 3.7 barns. The validity of this in the case of a liquid sample is questionable. (Also, the energy may not yet be low enough to eliminate the last Bragg reflection if the sample is a solid.)

Using the slope of the formula for the σ as given above, the absorption cross section at 2200 m/sec (0.0253 ev) is 2.2 barns, which is somewhat lower than the value of 2.71±0.12 given in AECU-2040.[4]

Figure 21 shows that there are no levels until the large level at about 100 ev. Below this, the curve is essentially $\sigma=7.3+0.35E^{-\frac{1}{2}}$, although as the level is approached, the transmission rises before dropping at the level.

Two clearly resolved levels at 102 ev and 310 ev are shown in Fig. 22. There are indications of levels at 500 ev and 1000 ev. It is difficult to make accurate calculations on the levels at 102 and 310 ev because the low

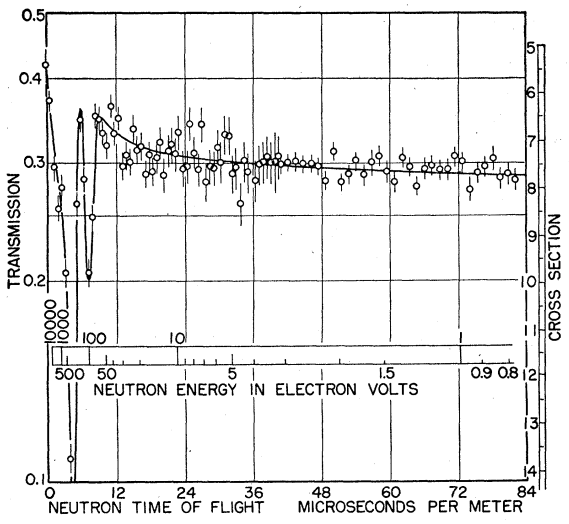

FIG. 21. The slow neutron transmission of 18.74 g/cm² of Ga with better resolution.

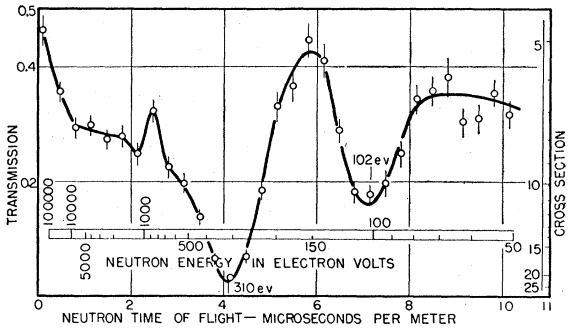

FIG. 22. The slow neutron transmission of 18.74g/cm² of Ga showing the two levels at 102 ev and 310 ev.

transmission (0.3–0.4) away from the levels makes it difficult to separate out the effect of the "background" portion of the cross section and also gives a large interference effect between the potential and resonant scattering terms. However, the area method was used to obtain approximate values of $\sigma_0\Gamma^2$. If $\Gamma_\gamma=0.1$ ev is assumed, we can get values for Γ_n and Γ by using the relationship $\sigma_0=4\pi\lambda^2 f(\Gamma_n/\Gamma)$, where f is taken as $\frac{1}{4}$ on the average. (f has the following four possible values, with spin$=\frac{3}{2}$ for both isotopes,

$$A=69: \quad f=0.229,\ 0.382;$$
$$A=71: \quad f=0.145,\ 0.242.)$$

The results are given in Table V.

TABLE V

E_0 (ev)	$\sigma_0\Gamma^2$ (b-ev²)	Γ (ev)	Γ_n (ev)	σ_0 (b)	σ_{0c} (b)	$\Gamma_n E^{-\frac{1}{2}}$ (ev$^{\frac{1}{2}}$)	$\sigma_{0c}\Gamma^2/4E_0^{\frac{3}{2}}$ (b-ev$^{\frac{1}{2}}$)
120	2200	0.71	0.61	6000	900	0.056	0.063
310	170 000	9.0	8.9	2100	23	0.50	0.086
						Sum:	0.149

The last column gives the predicted value for the thermal $E^{-\frac{1}{2}}$ slope on the bases of these two levels alone. The result is less than half of the measured value of 0.35. The difference may be due to the other levels and to negative levels. However, the calculations are sufficiently crude that anything better than order of magnitude agreement is not to be expected.

These data are essentially in agreement with the Harwell data (AECU-2040),[4] although there are some differences. In particular, the 102-ev level is found by the Harwell group to be at 95 ev and somewhat narrower.

The authors wish to express their appreciation to Miriam Levin for her extremely valuable assistance in taking, plotting, and analyzing the data. We also wish to acknowledge the assistance of Edward Stone and Murray Weinstein for computational help in the calculation of the Doppler effect. We wish to thank Jules Levin of the Brookhaven National Laboratory for his helpful criticism and valuable suggestions. Appreciation is also expressed to the U. S. Atomic Energy Commission for their financial support and interest in this research.